Catalysis of Hydrolysis and Nucleophilic Substitution at the P–N Bond of Phosphoimidazolide-Activated Nucleotides in Phosphate Buffers

Anastassia Kanavarioti* and Morgan T. Rosenbach

Chemistry Department, University of California, Santa Cruz, California 95064

Received June 5, 1990

Phosphoimidazolide-activated derivatives of guanosine and cytidine 5′-monophosphates, henceforth called ImpN's, exhibit enhanced rates of degradation in the presence of aqueous inorganic phosphate in the range $4.0 \leq pH \leq 8.6$. This degradation is been attributed to (i) nucleophilic substitution of the imidazolide and (ii) catalysis of the P–N bond hydrolysis by phosphate. The first reaction results in the formation of nucleoside 5′-diphosphate and the second in nucleoside 5′-monophosphate. Analysis of the observed rates as well as the product ratios as a function of pH and phosphate concentration allow distinction between various mechanistic possibilities. The results show that both $H_2PO_4^-$ and HPO_4^{2-} participate in both hydrolysis and nucleophilic substitution. Statistically corrected bimolecular rate constants indicate that the dianion is 4 times more effective as a general base than the monoanion, and 8 times more effective as nucleophile. The low Bronsted value $\beta = 0.15$ calculated for these phosphate species, presumed to act as general bases in facilitating water attack, is consistent with the fact that catalysis of the hydrolysis of the P–N bond in ImpN's has not been detected before. The $\beta_{nuc} = 0.35$ calculated for water, $H_2PO_4^-$, HPO_4^{2-}, and hydroxide acting as nucleophiles indicates a more associative transition state for nucleotidyl (O_2POR^- with R = nucleoside) transfers than that observed for phosphoryl (PO_3^{2-}) transfers ($\beta_{nuc} = 0.25$). With respect to the stability/reactivity of ImpN's under prebiotic conditions, our study shows that these materials would not suffer additional degradation due to inorganic phosphate, assuming the concentrations of phosphate, P_i, on prebiotic Earth were similar to those in the present oceans ($[P_i] \approx 2.25\ \mu M$).

Introduction

Nucleotide triphosphates, like ATP and GTP, are used in living cells both as an energy source in metabolism and as building blocks in polynucleotide synthesis. In the presence of an RNA or DNA molecule acting as the template, these activated mononucleotides polymerize to form a polynucleotide complementary to the template. The complementarity is achieved via Watson–Crick base interactions which specify that guanosine hydrogen bonds with cytosine, and adenine with uracil in RNA, or thymine in DNA.[1] This complementarity then results in information transfer from one generation of molecules to the next.

It is presumed that at an early stage of evolution and in the absence of a sophisticated enzyme machinery, template-directed reactions of nucleotides or nucleotide analogues may have been responsible for some "primitive" polynucleotide synthesis and information transfer.[2] Therefore a substantial effort has been devoted to the study of these reactions under a variety of conditions, but in the absence of enzymes. Nucleotide triphosphates, abbreviated pppN (see structures), have a high energy content, but they are kinetically very stable. In the contemporary cell this sluggishness is overcome by the action of enzymes. In the absence of enzymes the reactivity can be enhanced by using ImpN's, an approach which has been frequently used.[3]

We have studied the reactions of ImpN's both in the presence and in the absence of an appropriate template in water. Most of the studies were focused on the reactions of guanosine 5′-phosphate 2-methylimidazolide, 2-MeImpG. In the presence of the template polycytidylate, poly(C), this monomer polymerizes quantitatively and forms oligoguanylates that are up to 40 units long.[4] In the absence of poly(C), 2-MeImpG hydrolyzes at the P–N bond to form guanosine 5′-phosphate, 5′-GMP, and 2-methylimidazole, 2-MeIm.[5] Other ImpN's hydrolyze in a similar manner. Hydrolysis rate constants are largely independent of the nucleobase N.[6]

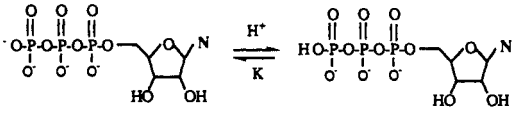

triphosphate nucleotides (e.g. GTP, CTP) pppN

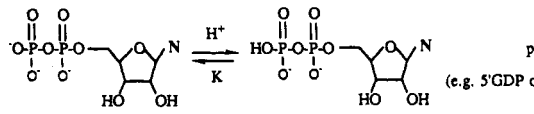

ppN (e.g. 5'GDP or 5'CDP)

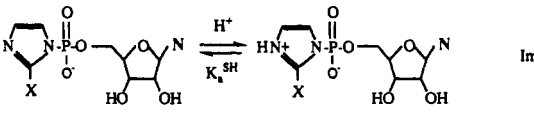

ImpN

S⁻ SH±

(e.g. with X=H, ImpG or ImpC; with X=Me, 2-MeImpG or 2-MeImpC)

for guanine (G-) derivatives

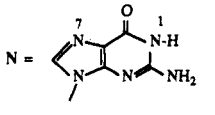

for cytosine (C-) derivatives

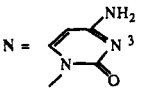

Ionization constants, K's, are all in the range $6 < pK < 8$.[6,7] At $pH < pK_a^{SH}$ (ImpN ionization constant, pK_a^{SH}, similar to the pK_a of the imidazole leaving group) the rate of ImpN hydrolysis depends on the pK_a of the imidazole derivative, but is pH independent. At $pH > pK_a^{SH}$ hydrolysis is independent of pK_a, decreases with increasing pH up to a point but accelerates again in highly basic solutions.[6]

(1) Watson, J. D.; Crick, F. H. C. *Nature* **1953**, *171*, 737.
(2) Orgel, L. E. *J. Theor. Biol.* **1986**, *123*, 127.
(3) Inoue, T.; Orgel, L. E. *Science* **1983**, *219*, 859. Schwartz, A. W.; Orgel, L. E. *Science* **1985**, *228*, 585.
(4) Inoue, T.; Orgel, L. E. *J. Mol. Biol.* **1982**, *162*, 201. Kanavarioti, A.; White, D. H. *Origins Life* **1987**, *17*, 333. Fakhrai, H.; Inoue, T.; Orgel, L. E. *Tetrahedron* **1984**, *40*, 39.
(5) Kanavarioti, A. *Origins Life* **1986**, *17*, 85.
(6) Kanavarioti, A.; Bernasconi, C. F.; Doodokyan, L. D.; Alberas, D. J. *J. Am. Chem. Soc.* **1989**, *111*, 7247.
(7) Phillips, R. S. J.; Eisenberg, P.; George, P.; Rutman, R. J. *J. Biol. Chem.* **1965**, *240*, 4393.

0022-3263/91/1956-1513$02.50/0

Significant dimerization of 2-MeImpG, although not the major reaction, occurs in concentrated solutions both in the presence and in the absence of poly(C); at initial concentrations of 0.05 and 0.07 M 2-MeImpG, approximately 20% ends up as dimer at 37 °C, ionic strength 1.75 M with NaCl and in the presence of 0.2 M $MgCl_2$.[8] Dimerization results in the formation of the three possible dimers, $(pG)_2^{3'-5'}$ and $(pG)_2^{2'-5'}$ and guanosine 5'-pyrophosphate-5'-guanosine (GppG).[8] The isomeric dimers $(pG)_2^{3'-5'}$ and $(pG)_2^{2'-5'}$ are most likely formed by nucleophilic reaction of the 3'-OH or the 2'-OH group of the ribose moiety of one monomer at the P–N bond of another monomer, with concurrent expulsion of the 2-methylimidazole leaving group. The major pathway(s) for the synthesis of GppG are not well established yet, but it seems clear that GppG must be formed by the nucleophilic reaction of a phosphate oxyanion of one monomer (hydrolyzed or unhydrolyzed) with the P–N bond of another monomer. Although these reactions are responsible for the dimerization and consequently the polymerization in the presence of a template, they have not been adequately studied.

As part of a research program aimed at investigating nucleophilic substitutions at the P–N bond of ImpN's, we now report such a study with 2-MeImpG in aqueous phosphate buffers. Our investigation shows that phosphate acts (a) as a general base catalyst in the hydrolysis and (b) as a nucleophile to replace the imidazole derivative (eq 1). Since the nucleophilic substitution results in the formation of a pyrophosphate bond, it can be regarded as a model reaction for the formation of dinucleotides such as GppG, or even pyrophosphate-capped oligonucleotides. In addition we report here that other ImpN's, such as guanosine 5'-phosphate imidazolide (ImpG), cytidine 5'-phosphate 2-methylimidazolide (2-MeImpC) and cytidine 5'-phosphate imidazolide (ImpC) react in similar manner and form diphosphate nucleotides (ppN's). The study of phosphoimidazolide activated nucleotides in the presence of phosphate is interesting in its own right because the stability/reactivity of these compounds in the presence of prebiotic materials such as inorganic phosphate should be evaluated.

Experimental Section

A. Materials. Solvents used were HPLC quality. Buffers and other reagents were purchased from Sigma or Aldrich, and they are abbreviated as follows: phosphate, P_i; imidazole, Im; 2-methylimidazole, 2-MeIm; guanosine 5'-phosphate, 5'-GMP; guanosine 5'-diphosphate, 5'-GDP; cytidine 5'-phosphate, 5'-CMP; cytidine 5'-diphosphate, 5'-CDP; *N*-(2-hydroxyethyl)piperazine-*N*'-2-ethanesulfonic acid, HEPES; 2-(*N*-morpholino)ethanesulfonic acid, MES. The sodium salts of the buffers were used. The sodium salts of 2-MeImpG, ImpG, 2-MeImpC, and ImpC were synthesized according to a known procedure.[9] The preparations were 95% pure as shown by HPLC.[10]

B. Kinetics. Samples were prepared in HPLC grade water. They contained 1 mM of the activated nucleotide and the desired amount of buffer and were brought to 1.75 M ionic strength with NaCl. The low concentration of nucleotide (1 mM) was chosen in order to suppress dimerization. The reactions were run at 37 ± 0.5 °C. Samples of 1000 μL prepared in 1.5 mL of polypropylene (Fisherbrand) test tubes were transferred directly into the HPLC vials. The vials were placed inside the thermostated autosampler of a 1090M Hewlett-Packard liquid chromatograph in which the analyses were carried out. UV absorbances were monitored at 254 nm with the G-derivatives and 270 nm with the C-derivatives. The absorbance observed in this region comes from the nucleotide moiety; imidazoles, Im and 2-MeIm, do not absorb. Most of the reactions were monitored for up to 5 half-lives, and first-order kinetics were obtained. Hence, first-order kinetics were presumed for the slower reactions that were run for 1 half-life only.

Analysis was performed using a 20-cm reversed-phase Hypersil ODS 5-μm column. Chromatographic conditions were modified from a previous method[10] and were as follows. Mobile phase: solvent A, 0.02 M potassium dihydrogen phosphate (pH 6.5); solvent B, acetonitrile–water (30:70). Gradient elution, 0–30% B in 13 min. Under our analytical conditions retention times (in minutes) of the nucleotides are as follows: ImpG, 11.2; 2-MeImpG, 10.3; ImpC, 10.4; 2-MeImpC, 9.4; 5'-GMP, 3.7; 5'-GDP 2.7; 5'-CMP, 2.65; 5'-CDP, 2.4.

Rate constants, k_{obsd}, in h^{-1}, were calculated from the slope of a plot of ln (HPLC area of the imidazolide substrate) as a function of time using least-squares analysis. For the determination of each rate constant 10–15 aliquots of the same sample were used and the standard error for any given sample was less than 5%, as shown by repeating experiments (see Table II). Similarly, the standard error for product ratios was less than 12%. The pH was measured at room temperature either in mock solutions excluding the substrate, or directly in the test tubes using a microelectrode (MI 410 by Microelectrodes, Inc.). At the extreme ends of the pH range it was necessary to adjust the pH of some of the buffers in order to keep pH constancy within a series of variable buffer concentration.

Results and Discussion

The hydrolysis of 2-MeImpG to form 2-methylimidazole and the unreactive 5'-GMP has been studied in detail in a pH range of $1 < pH < 12$ in water.[5,6] Peaks representing both substrate and product are present in a typical HPLC chromatogram. Some of the buffers used to study the hydrolysis reaction exhibited a small rate-enhancing effect as a function of buffer concentration; this will be discussed later. However, these buffers did not react with ImpN as shown by the absence of any additional peak in the HPLC chromatograms. Therefore their rate-enhancing effect is attributed to buffer catalysis of the P–N bond hydrolysis. In contrast to this behavior, reaction of 2-MeImpG in phosphate buffers was characterized by (i) an accelerated disappearance of the substrate as compared with the reaction under similar conditions but in the presence of other buffers and (ii) appearance of an additional product which was shown by coinjection with authentic material to be guanosine 5'-diphosphate, 5'-GDP. Representative experiments with other ImpN's in the presence of inorganic phosphate also indicated the formation of the corresponding diphosphate nucleotide.

1. Mechanism of Nucleophilic Substitution at the P–N Bond by Phosphate. The reaction of 2-MeImpG in aqueous phosphate buffers was studied at 37 °C in the range $4.02 \leq pH \leq 8.64$, and the ionic strength was kept constant at $\mu = 1.75$ with NaCl. The effect of phosphate buffer concentration was investigated in the range $0.05\ M \leq [P_i] \leq 0.50\ M$ with $[P_i]$ being the total inorganic phosphate concentration. Rates were determined by monitoring the disappearance of the substrate. Product distributions, i.e., the ratio [5'-GMP]/[5'-GDP], were determined directly from the HPLC areas of the corresponding peaks because these two molecules exhibit identical extinction coefficients at 254 nm, $\epsilon\ 1.37 \times 10^4$.[11] Table I summarizes all the data obtained in phosphate buffers, whereas Table II includes the data obtained with phosphate but in the presence of 0.10 and 0.40 M 2-MeIm buffers at pH 8.22 and 8.64, and in the presence of 0.02

(8) Kanavarioti, A.; Alberas, D. J.; Chang, S. *J. Mol. Evol.* **1990**, *31*, 462.
(9) Joyce, G. F.; Inoue, T.; Orgel, L. E. *J. Mol. Biol.* **1984**, *176*, 279.
(10) Kanavarioti, A.; Doodokyan, L. D. *J. Chromatogr.* **1987**, *389*, 334.
(11) 1.37×10^4 reported for GTP, GDP, GMP, and guanosine at 252 nm and pH 7: Volkin, E.; Cohn, W. E. *Methods of Biochemical Analysis*; Glick, D., Ed.; Interscience: New York, 1954.

Table I. Kinetics and Product Distribution of the Reaction of 2-MeImpG in Phosphate Buffers at 37 °C

pH	$[P_i]$, M	$10^2 k_{obsd}$, h^{-1}	[5′-GMP]/[5′-GDP][a]
4.65	0.10	4.26	7.30
	0.20	4.97	4.11
	0.30	5.60	3.10
	0.40	6.20	2.55
	0.50	6.76	2.31
4.95	0.10	4.40	5.77
	0.20	5.28	3.14
	0.30	6.05	2.41
	0.40	6.78	2.12
	0.50	7.45	1.91
5.53	0.05	4.76	4.87
	0.10	5.19	3.02
	0.20	6.89	1.68
	0.30	8.62	1.30
	0.40	9.66	1.15
	0.50	10.63	1.05
5.88	0.05	5.04	4.47
	0.10	6.13	2.60
	0.20	8.33	1.60
	0.30	10.44	1.27
	0.40	12.16	1.12
	0.50	13.67	1.02
6.16	0.05	4.18	3.15
	0.10	5.41	1.78
	0.20	7.27	1.17
	0.30	9.72	1.05
6.86	0.05	2.49	2.39
	0.10	3.97	1.39
	0.20	5.98	0.99
	0.30	8.69	0.72
7.30	0.05	1.40	2.19
	0.10	1.89	1.27
	0.20	3.64	0.85
	0.30	5.60	0.76
7.42	0.05	1.86	2.15
	0.08	2.30	1.55
	0.10	2.68	1.32
	0.20	4.11	0.90
	0.30	5.56	0.79
	0.40	7.10	0.75
8.22[b]	0.05	0.387	2.08
	0.10	0.531	1.45
	0.20	1.01	0.87
	0.40	1.49	0.70
8.64[b]	0.05	0.186	2.94
	0.10	0.249	1.85
	0.20	0.376	1.04
	0.40	0.750	0.85

[a] [5′-GMP]/[5′-GDP] = [5′-GMP] − [5′-GMP]$_0$/[5′-GDP] − [5′-GDP]$_0$ is the product distribution as obtained from the HPLC areas of the corresponding peaks, but corrected for the presence of some material, [5′-GMP]$_0$ and [5′-GDP]$_0$, at zero time. [b] Rate constants and product ratios extrapolated from 0.1 and 0.4 M 2-MeIm buffers (see Table II).

M acetate at pH 4.02 and 4.26. Extrapolation to zero buffer concentration with the 2-MeIm buffers was necessary because of a small catalysis observed by 2-MeIm. Extrapolated values for k_{obsd} and product ratios are presented in Table I.

The following conclusions can be drawn by inspection of Table I. Rates for the disappearance of 2-MeImpG increase and the product ratio [5′-GDP]/[5′-GMP] increases, or [5′-GMP]/[5′-GDP] decreases with buffer concentration over the entire pH range studied (Table I). These observations are consistent with nucleophilic substitution of 2-methylimidazole by phosphate to form 5′-GDP. Representative data taken from Table I are illustrated as plots of k_{obsd} as a function of phosphate buffer concentration (Figure 1). Figure 1 includes data in the high pH region: at pH 6.86, 7.42, 8.22, and 8.64. It is seen that the slopes of the plots in the high pH region decrease

Table II. Kinetics and Product Distribution of the Reaction of 2-MeImpG with Phosphate in Acetate Buffers at pH 4.02 and 4.26 and in 2-Methylimidazole Buffers at pH 8.22 and 8.64 at 37 °C

pH	$[2\text{-MeIm}]_{tot}$, M or $[acetate]_{tot}$, M	$[P_i]$, M	$10^2 k_{obsd}$, h^{-1}	[5′-GMP]/[5′-GDP][a]
4.02	0.02	0.02	3.51	>80
		0.05	3.63	>20
		0.10	3.91	11.71
		0.10	4.30	9.17
		0.15	4.15	8.14
		0.20	4.52	6.44
		0.20	4.88	5.08
		0.30	5.33	3.70
		0.40	6.01	3.14
		0.50	6.49	2.96
4.26	0.02	0.02	3.57	>30
		0.05	3.84	18.40
		0.10	4.00	9.92
		0.10	4.08	9.70
		0.15	4.24	6.76
		0.20	4.54	5.21
		0.20	4.87	5.43
		0.30	5.39	4.02
		0.40	5.89	3.27
		0.50	6.26	2.88
8.22	0.10	0.05	0.430	2.50
		0.10	0.576	1.70
		0.20	1.029	1.01
		0.40	1.541	0.78
8.22	0.40	0.05	0.558	6.25
		0.10	0.710	3.33
		0.20	1.080	2.00
		0.40	1.682	1.19
8.64	0.10	0.05	0.205	3.13
		0.10	0.268	2.00
		0.20	0.398	1.15
		0.40	0.750	0.89
8.64	0.40	0.05	0.261	3.85
		0.10	0.325	2.63
		0.20	0.463	1.67
		0.40	0.729	1.02

[a] As in Table I.

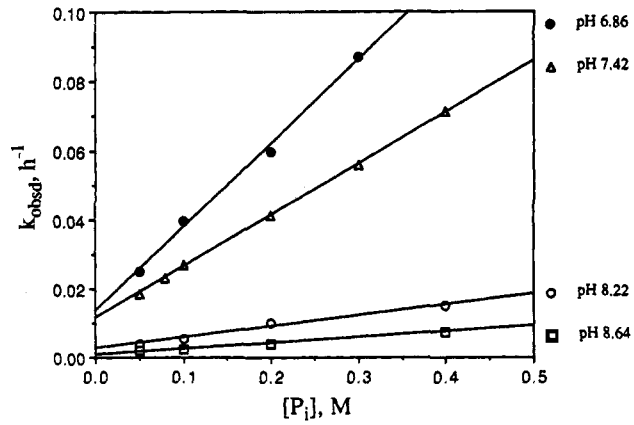

Figure 1. The effect of the concentration of phosphate buffer on the rate constant for disappearance of 2-MeImpG in the basic pH region at 37 °C and ionic strength 1.75 with NaCl.

with increasing pH (Figure 1) whereas the opposite is true in the low pH region. The largest slope is observed at pH ≈ 6.8. Plots of k_{obsd} vs $[P_i]$ provide intercepts and slopes abbreviated I_k^P and S_k, respectively. I_k^P and S_k at each pH studied are reported in Table III. However, because of the strong buffer dependence of the rate on phosphate concentration, the intercepts of the buffer plots, I_k^P, have a relatively high experimental error. Much better values for intercepts, abbreviated I_k, can be obtained from the experiments in MES and 2-MeIm buffers (see later under 2). Indeed these experiments allow the determination of

Table III. Analysis of Plots of k_{obsd} (h^{-1}) vs $[P_i]$ (M) and of Product Distributions [5′-GMP]/[5′-GDP] vs $1/[P_i]$ (M^{-1}) for 2-MeImpG

pH	I_k^P,[a] h^{-1}	S_k,[a] M^{-1} h^{-1}	I_k,[b] h^{-1}	S_k/I_k	I_p,[c]	S_p,[c] M
4.02	3.38×10^{-2}	0.064	3.32×10^{-2}	1.93	0.854	0.980
4.26	3.48×10^{-2}	0.058	3.31×10^{-2}	1.75	1.075	0.866
4.65	3.69×10^{-2}	0.062	3.31×10^{-2}	1.87	1.007	0.628
4.95	3.71×10^{-2}	0.076	3.30×10^{-2}	2.30	0.851	0.486
5.53	4.09×10^{-2}	0.137	3.23×10^{-2}	4.24	0.635	0.216
5.88	4.28×10^{-2}	0.194	3.13×10^{-2}	6.20	0.641	0.192
6.16	3.12×10^{-2}	0.217	2.97×10^{-2}	7.31	0.559	0.128
6.86	1.36×10^{-2}	0.242	2.09×10^{-2}	11.58	0.439	0.097
7.30	1.17×10^{-2}	0.171	1.27×10^{-2}	13.46	0.433	0.087
7.42	1.14×10^{-2}	0.149	1.06×10^{-2}	14.06	0.520	0.081
8.22	2.56×10^{-3}	0.032	2.29×10^{-3}	13.97	0.524	0.080
8.64	8.58×10^{-4}	0.016	9.10×10^{-4}	17.58	0.522	0.122
4.70[d]	0.628	1.935		3.08[g]	0.328	0.661
4.70[e]	0.899	1.958		2.18[g]	0.812	0.548
4.70[f]	4.54×10^{-2}	0.083		1.83[g]	0.916	0.718

[a] I_k^P and S_k refer to the intercept and slope respectively of the least-squares analysis of a plot of k_{obsd} vs total phosphate concentration. [b] $I_k = a_H k_h^w/(a_H + K_a^{SH})$, where a_H is the hydrogen activity, $k_{SH}^w = 3.32 \times 10^{-2}$ h^{-1}, and $K_a^{SH} = 8.13 \times 10^{-8}$ M^{-1}; both values obtained from experiments with MES and 2-MeIm buffers (see under 2). [c] I_p and S_p refer to the intercept and slope respectively of the least-squares analysis of a plot of product distribution [5′-GMP]/[5′-GDP] vs $1/[P_i]$. [d] Analysis of the data for the reaction of ImpG with phosphate. [e] As in *d* with ImpC and products 5′-CMP and 5′-GDP. [f] As in *e* with 2-MeImpC. [g] Ratios corresponds to S_k/I_k^P.

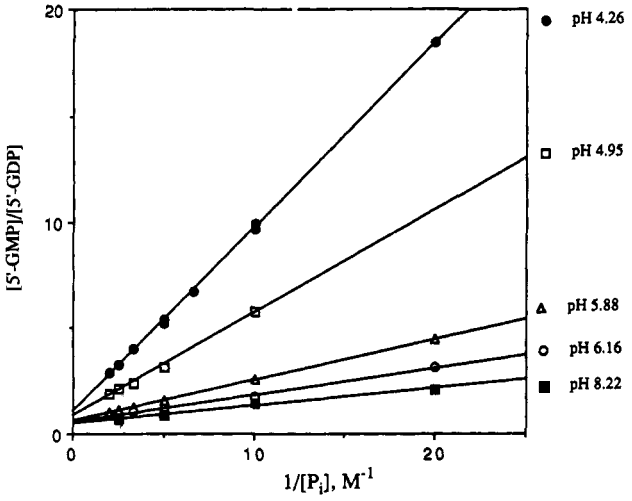

Figure 2. The effect of the concentration of phosphate buffer on the product ratio [5′-GMP]/[5′-GDP] as a function of pH.

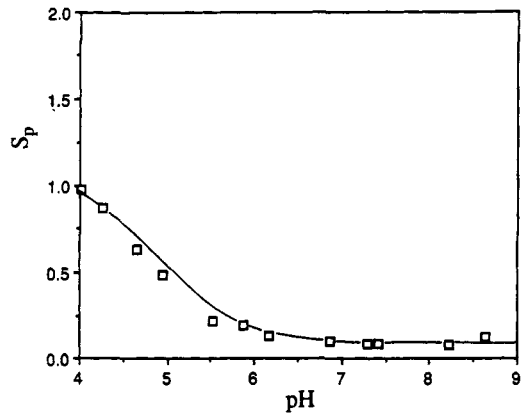

Figure 3. The effect of pH on S_p. S_p refers to the slope of a plot of [5′-GMP]/[5′-GDP] vs $1/[P_i]$; data obtained from Table III. The solid line is calculated from the S_p expression of mechanism 11 (Table IV) and the determined rate and equilibrium constants.

$K_a^{SH} = 8.13 \times 10^{-8}$ M^{-1} and $k_{SH}^w = 3.32 \times 10^{-2}$ h^{-1}. I_k is then calculated from $I_k = a_H k_{SH}^w/(a_H + K_a^{SH})$,[6] where a_H is the hydrogen activity. Values of I_k (not very different from I_k^P) at various pH's have been included in Table III and were used to calculate S_k/I_k. The latter will be useful in our analysis of the various mechanistic possibilities.

Plots (not shown) of [5′-GDP]/[5′-GMP] as a function of $[P_i]$ exhibit curvilinear behavior. However, straight lines are obtained by plotting [5′-GMP]/[5′-GDP] vs $1/[P_i]$. Representative plots are illustrated in Figure 2. It is seen that these plots have finite intercepts and slopes increasing with decreasing pH. Both slopes and intercepts seem to converge in the high pH region. Plots of [5′-GMP]/[5′-GDP] vs $1/[P_i]$ provide intercepts and slopes abbreviated I_p and S_p, respectively, and are reported in Table III.

The mechanism of the hydrolysis of ImpN's, established earlier, calls for a preequilibrium between the unprotonated substrate (S^-, see structures) and the zwitterionic form ($SH^\pm$) which is the reactive species in the pH range studied here.[6] In analogy to the hydrolysis mechanism, we postulate that nucleophilic substitution by phosphate can only occur on $SH^\pm$. Considering the fact that the monoanion, P^-, and dianion, P^{2-}, are the only phosphate species present in considerable amount in solutions in the pH range studied, one can postulate up to 11 different mechanistic possibilities to describe the formation of the two reaction products. The reaction of $SH^\pm$ with OH^- is not very important even at the highest pH = 8.6, as established in a previous study.[6] The different mechanisms are abbreviated by indicating the catalysts for the hydrolysis reaction followed by the nucleophiles for the formation of the diphosphate. For example, a mechanism that includes catalysis of the hydrolysis by the monoanion and nucleophilic substitution by both the monoanion and the dianion is abbreviated W, P^-/P^-, P^{2-}.

A list of all possible mechanisms and their corresponding expressions I_p, S_p, and S_k/I_k as obtained from the appropriate rate law and product distribution equations (not included) are presented in Table IV. Replacing I_k and S_k with S_k/I_k as mechanistic criterion is justified because both I_k and S_k are proportional to the preequilibrium factor $a_H/(a_H + K_a^{SH})$, whereas parameter S_k/I_k is independent of this preequilibrium and therefore normalized. It was necessary to propose involvement by both phosphate monoanion and dianion on both nucleophilic and general base catalyzed pathways. The proposed mechanism is illustrated in eq 1. It obeys the rate law given by eq 2 and exhibits product ratio given by eq 3. S^- and $SH^\pm$ represent

$$S^- \underset{K_a^{SH}}{\overset{H^+}{\rightleftharpoons}} SH^\pm \begin{cases} \xrightarrow{k_h^w + k_h^{P-}[H_2PO_4^-] + k_h^{P2-}[HPO_4^{2-}]} 5'\text{-GMP} \\ \xrightarrow{k_p^-[H_2PO_4^-] + k_p^{2-}[HPO_4^{2-}]} 5'\text{-GDP} \end{cases} \quad (1)$$

the unprotonated and protonated forms of 2-MeImpG,

Table IV. Analysis of All Possible Mechanisms for the Reaction of 2-MeImpG in the Presence of Phosphate Monoanion and Dianion (see Text for Explanation of Symbols)

no.	mechanism	I_p	S_p	S_k/I_k
1	W/P^-	0	$\frac{k_h^w}{k_p^-}\frac{(a_H + K_2^p)}{a_H}$	$\frac{k_p^- a_H}{k_h^w(a_H + K_2^p)}$
2	W/P^{2-}	0	$\frac{k_h^w}{k_p^{2-}}\frac{(a_H + K_2^p)}{K_2^p}$	$\frac{k_p^{2-}K_2^p}{k_h^w(a_H + K_2^p)}$
3	$W,P^-/P^{2-}$	$\frac{k_h^{p-}}{k_p^{2-}}\frac{a_H}{K_2^p}$	$\frac{k_h^w}{k_p^{2-}}\frac{(a_H + K_2^p)}{K_2^p}$	$\frac{k_h^{p-}a_H + k_p^{2-}K_2^p}{k_h^w(a_H + K_2^p)}$
4	$W,P^-/P^-$	$\frac{k_h^{p-}}{k_p^-}$	$\frac{k_h^w}{k_p^-}\frac{(a_H + K_2^p)}{a_H}$	$\frac{(k_h^{p-} + k_p^-)a_H}{k_h^w(a_H + K_2^p)}$
5	$W,P^{2-}/P^{2-}$	$\frac{k_h^{p2-}}{k_p^{2-}}$	$\frac{k_h^w}{k_p^{2-}}\frac{(a_H + K_2^p)}{K_2^p}$	$\frac{(k_h^{p2-} + k_p^{2-})a_H}{k_h^w(a_H + K_2^p)}$
6	$W,P^{2-}/P^-$	$\frac{k_h^{p2-}}{k_p^-}\frac{K_2^p}{a_H}$	$\frac{k_h^w}{k_p^-}\frac{(a_H + K_2^p)}{a_H}$	$\frac{k_p^- a_H + k_h^{p2-}K_2^p}{k_h^w(a_H + K_2^p)}$
7	$W,P^{2-},P^-/P^-$	$\frac{k_h^{p-}}{k_p^-} + \frac{k_h^{p2-}}{k_p^-}\frac{K_2^p}{a_H}$	$\frac{k_h^w}{k_p^-}\frac{(a_H + K_2^p)}{a_H}$	$\frac{(k_h^{p-} + k_p^-)a_H + k_h^{p2-}K_2^p}{k_h^w(a_H + K_2^p)}$
8	$W,P^{2-},P^-/P^{2-}$	$\frac{k_h^{p2-}}{k_p^{2-}} + \frac{k_h^{p-}}{k_p^{2-}}\frac{a_H}{K_2^p}$	$\frac{k_h^w}{k_p^{2-}}\frac{(a_H + K_2^p)}{K_2^p}$	$\frac{(k_h^{p2-} + k_p^{2-})K_2^p + k_h^{p-}a_H}{k_h^w(a_H + K_2^p)}$
9	$W,P^{2-}/P^-,P^{2-}$	$\frac{k_h^{p2-}K_2^p}{k_p^{2-}K_2^p + k_p^- a_H}$	$\frac{k_h^w(a_H + K_2^p)}{k_p^{2-}K_2^p + k_p^- a_H}$	$\frac{(k_h^{p2-} + k_p^{2-})K_2^p + k_p^- a_H}{k_h^w(a_H + K_2^p)}$
10	$W,P^-/P^-,P^{2-}$	$\frac{k_h^{p-}a_H}{k_p^{2-}K_2^p + k_p^- a_H}$	$\frac{k_h^w(a_H + K_2^p)}{k_p^{2-}K_2^p + k_p^- a_H}$	$\frac{(k_h^{p-} + k_p^-)a_H + k_p^{2-}K_2^p}{k_h^w(a_H + K_2^p)}$
11	$W,P^-,P^{2-}/P^-,P^{2-}$	$\frac{k_h^{p2-}K_2^p + k_h^{p-}a_H}{k_p^{2-}K_2^p + k_p^- a_H}$	$\frac{k_h^w(a_H + K_2^p)}{k_p^{2-}K_2^p + k_p^- a_H}$	$\frac{(k_H^{p-} + k_p^-)a_H + (k_h^{p2-} + k_p^{2-})K_2^p}{k_h^w(a_H + K_2^p)}$

proton located at the imidazolide moiety, with $K_a^{SH} = 8.13 \times 10^{-8}$ M^{-1} (see later under 2); $k_h^w = 3.32 \times 10^{-2}$ h^{-1} is the hydrolysis rate constant with water as the nucleophile; a_H is the hydrogen ion activity taken from the pH reading; k_h^{p-} and k_h^{p2-} represent the bimolecular rate constants for general base catalysis by the phosphate monoanion and dianion, respectively; k_p^- and k_p^{2-} represent the bimolecular rate constants for nucleophilic attack by the phosphate monoanion and dianion, respectively; K_2^p is the second ionization constant of phosphate $H_2PO_4^- \rightleftharpoons H^+ + HPO_4^{2-}$, $pK_2^p = 6.10$ under our conditions. In eqs 2 and 3 the concentrations of the monoanion and dianion have been replaced by $[H_2PO_4^-] = a_H[P_i]/(a_H + K_2^p)$ and $[HPO_4^{2-}] = K_2^p[P_i]/(a_H + K_2^p)$.

$$k_{obsd} = \frac{a_H}{a_H + K_a^{SH}}\left\{k_h^w + \frac{(k_h^{p-} + k_p^-)a_H + (k_h^{p2-} + k_p^{2-})K_2^p}{(a_H + K_2^p)}[P_i]\right\} \quad (2)$$

$$\frac{[5'\text{-GMP}]}{[5'\text{-GDP}]} = \frac{k_h^{p2-}K_2^p + k_h^{p-}a_H}{k_p^{2-}K_2^p + k_p^- a_H} + \frac{k_h^w(a_H + K_2^p)}{k_p^{2-}K_2^p + k_p^- a_H}\frac{1}{[P_i]} \quad (3)$$

A choice for mechanism 11 (eq 1) and against the other possibilities was made based on the fact that this is the only mechanism that is consistent with the pH dependence of all parameters I_p, S_p, and S_k/I_k. In order to simplify the comparison between predicted parameters and observations we have plotted S_p vs pH (Figure 3) and I_p vs pH (Figure 4). Both plots exhibit a similar sigmoidal

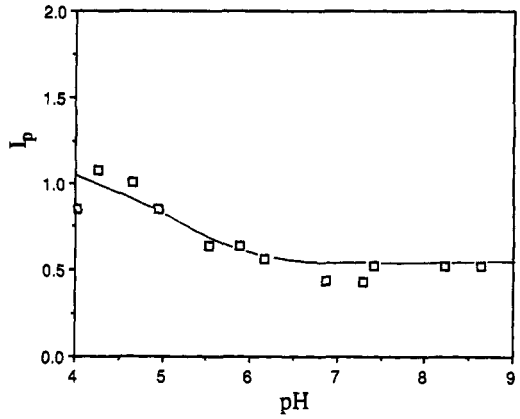

Figure 4. The effect of pH on I_p. I_p refers to the intercept of a plot of [5′-GMP]/[5′-GDP] vs 1/[P_i]; data obtained from Table III. The solid line is calculated from the I_p expression of mechanism 11 (Table IV) and the determined rate and equilibrium constants.

shape: At high pH S_p and I_p are independent of pH, increase with increasing a_H, and show the onset of a leveling off at low pH.

In trying to fit observed (Table III and Figure 3) with predicted behavior of parameter S_p as function of pH (Table IV) it can be seen that mechanisms 2, 3, 5, and 8 are inconsistent with the data because they predict that at low pH S_p should become proportional to a_H. Mechanisms 1, 4, 6, and 7 cannot describe our results either, because they predict that at high pH S_p should be inversely proportional to a_H. In contrast to that, the anticipated behavior of S_p as a function of pH *is* consistent with our data for mechanisms 9, 10, and 11 (same S_p expression).

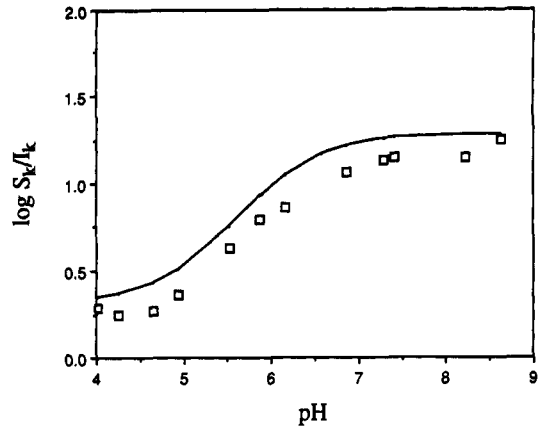

Figure 5. The effect of pH on the logarithm of S_k/I_k; data taken from Table III. S_k refers to the slope of a plot of k_{obsd} vs $[P_i]$ and I_k is the rate constant of reaction at zero buffer concentration. The solid line is calculated from S_k/I_k expression (Table IV) of mechanism 11 and the determined rate and equilibrium constants.

In this case S_p vs a_H is consistent with Figure 3 assuming that at low pH $k_p^- a_H \gg k_p^{2-} K_2^p$ and at high pH $k_p^- a_H \ll k_p^{2-} K_2^p$.

We will show how additional consideration of the predicted behavior of I_p as a function of pH enabled us to narrow down the mechanistic possibilities to just one. Indeed the expression of I_p does not predict a leveling off at low pH with mechanism 9 (assuming $k_p^{2-} K_2^p \ll k_p^- a_H$) and no leveling off at high pH with mechanism 10 (assuming $k_p^{2-} K_2^p \gg k_p^- a_H$). Incidentally, an inspection of the predicted I_p's in Table IV suggests that mechanisms 1–6 are inconsistent with our results because they predict that I_p is either equal to zero (mechanisms 1 and 2), a constant (mechanisms 4 and 5), proportional to a_H (mechanism 3), or inversely proportional to a_H (mechanism 6). Furthermore, mechanisms 7–9 predict a plot of I_p vs pH with no leveling off at the low pH range assuming that at pH $\ll pK_2^p$: $k_h^{p-} \ll k_h^{p2-} K_2^p / a_H$ with mechanism 7 and $k_h^{p2-} \ll k_h^{p-} a_H / K_2^p$ with mechanism 8. However, mechanism 11 predicts for I_p a behavior consistent with Figure 5 assuming that at low pH (pH ≈ 4) $k_h^{p-} a_H \gg k_h^{p2-} K_2^p$ and $k_p^- a_H \gg k_p^{2-} K_2^p$ and that at high pH (pH ≈ 8) the opposite inequalities apply. Hence mechanism 11 (eq 1, abbreviated W, P^-, P^{2-}/P^-, P^{2-}) including catalysis of the hydrolysis by both the monoanion and dianion, as well as nucleophilic reaction by both is the only mechanism out of eleven consistent with all the experimental data.

Bimolecular rate constants k_h^{p-}, k_h^{p2-}, k_p^-, and k_p^{2-} were obtained as follows: At pH $\gg pK_2^p$ the expressions for I_p and S_p (Table IV) can be simplified to $I_p \approx k_h^{p2-}/k_p^{2-}$ and $S_p \approx k_h^w/k_p^{2-}$. In other words, the extended plateau obtained with I_p and S_p at pH > 6 indicates that the reaction can be approximated by the simplified mechanism W, P^{2-}/P^{2-}. At pH ≥ 7.42 we note from Table III that I_p = 0.522 and S_p = 0.080 M. Using $k_h^w = 3.32 \times 10^{-2}$ h^{-1} one calculates $k_p^{2-} = 0.415$ M^{-1} h^{-1} and $k_h^{p2-} = 0.217$ M^{-1} h^{-1}. Then $k_p^- = 3.35 \times 10^{-2}$ M^{-1} h^{-1} is obtained as the value with the best least-squares analysis fit of the S_p data for the whole pH range using the full expression for S_p (S_p in Table IV for mechanism 11 or the P_i-dependent part of eq 6). Similarly, $k_h^{p-} = 3.61 \times 10^{-2}$ M^{-1} h^{-1} is obtained as the value that gives the best fit of the I_p data solving the full expression of I_p after substituting all the other rate constants (I_p in Table IV for mechanism 11 or the P_i-independent part of eq 3).

The solid lines drawn in Figures 3 and 4, which were generated from the rate constants obtained by the described procedures, show a very good fit with the experimental data. The fit between experimental and calculated S_k/I_k ratios (Figure 5) is not as good as for the I_p and S_p plots but still quite satisfactory, with most of the deviations being less than 0.15 log units (41%). Incidentally, the fit between the calculated and experimental S_k/I_k ratios is a small improvement over the corresponding fit with the S_k/I_k^p ratios. One plausible reason for these deviations is a salt effect that is caused by a different mix of phosphate salts and the compensating electrolyte. This salt effect would affect data at high phosphate concentration differently than data at low phosphate concentration and maybe result in a diminished S_k. An involvement by PO_4^{3-}, as suggested by a reviewer, although possibly relevant at pH ≫ 8.4, would not explain the deviation of S_k/I_k in the range 4 < pH < 8.6. This is shown by the following calculations: Based on the low values of β and β_{nuc} (see later) one can predict that at pH 8.6 $[PO_4^{3-}] = 0.025[P_i]_{tot}$ with a potential contribution to the rate of up to 12%, assuming $pK_3^p = 10$ (K_3^p the third ionization constant of phosphate), and $[PO_4^{3-}] = 0.0025[P_i]_{tot}$ with a contribution of only 3% assuming $pK_3^p = 11$.[12] Hence, PO_4^{3-} may contribute to the rate 3–12% at pH 8.6 and decreasingly less with pH < 8.6.

We interpret the phosphate catalysis as general base assisted water attack with a transition state possibly like **1**, whereas the transition state for the nucleophilic substitution may be represented by **2**.

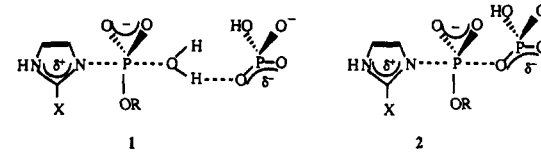

1 **2**

Table V. Second-Order Rate Constants for Reactions of the Zwitterionic 2-MeImpG with Oxygen Nucleophiles

nucleophile	pK_a	$pK_a + \log p/q^a$	k, M^{-1} h^{-1}	$\log k/q^a$
H_2O^b	−1.74	−1.26	$k_h^w = 0.0332/55$	−3.22
$H_2PO_4^-$	1.72	1.90	$k_p^- = 0.0335$	−1.78
HPO_4^{2-}	6.10	5.92	$k_p^{2-} = 0.415$	−0.86
OH^{-b}	15.42	15.72	$k_h^{OH} = 952$	2.98
gen. base				
$H_2PO_4^-$	1.72	1.90	$k_h^{p-} = 0.0361$	−1.74
HPO_4^{2-}	6.10	5.92	$k_h^{p2-} = 0.217$	−1.14

[a] q = number of basic sites on the general base, p = number of protons on the conjugate general acid. [b] These reactions were studied in ref 6; $k_h^{OH} = k_{SH}^{OH}$ in ref 6; see also in Table VIII, this paper.

Table V includes bimolecular rate constants k_p^- and k_p^{2-} for $H_2PO_4^-$ and HPO_4^{2-} obtained in this study as well as k_h^w and k_h^{OH} for water and hydroxyl anion obtained in an earlier study.[6] A plot (not shown) of the logarithms of the rate constants of the nucleophiles (water, $H_2PO_4^-$, HPO_4^{2-}, and OH^-) with their pK_a's exhibits a surprisingly linear correlation with a slope $\beta_{nuc} = (d \log k)/(d\ pK_{nuc}) = 0.35$. This value is higher than $\beta_{nuc} \approx 0.25$ observed for phosphoryl transfers.[13] In our study the place of the phosphoryl (PO_3^{2-}) is taken by a nucleotidyl group (O_2POR^- with R = nucleoside), i.e., a singly substituted phosphoryl group. The nucleotidyl has one negative charge less than the phosphoryl group that results in strongly diminished

(12) pK_3^p is not known at 37 °C and μ = 1.75 M (NaCl), estimated to be 10 < pK_3^p < 11. Because of the higher ionic strength used in our experiments pK_3^p should be lower than 12.67 (thermodynamic value at 18 °C) and even lower than 11.44 (at 30 °C, μ = 1.0 M from Bruice, P. Y. *J. Am. Chem. Soc.* **1984**, *106*, 5959).

(13) Herschlag, D.; Jencks, W. P. *J. Am. Chem. Soc.* **1990**, *112*, 1942. Herschlag, D.; Jencks, W. P. *J. Am. Chem. Soc.* **1989**, *111*, 7587.

Table VI. Kinetics of the Hydrolysis of 2-MeImpG in MES Buffers at 37 °C

pH	$[MES]_{tot}$, M	10^2k_{obsd}, h^{-1}	10^2k_{obsd}, h^{-1} average
5.61	0.20	3.23	
	0.30	3.30	
	0.40	3.31	3.28 ● 0.05
6.02	0.10	3.19	
	0.20	3.22	
	0.30	3.20	
	0.40	3.21	3.20 ● 0.02
6.44	0.10	2.87	
	0.20	2.86	
	0.30	2.89	
	0.40	2.90	2.88 ± 0.02
6.68	0.10	2.79	
	0.30	2.93	
	0.40	2.76	2.83 ± 0.10
7.16	0.20	1.75	
	0.30	1.83	
	0.40	1.80	1.79 ● 0.04
7.29	0.05	1.42	
	0.10	1.49	
	0.20	1.66	
	0.30	1.51	
	0.40	1.50	1.52 ± 0.14

electrostatic repulsion with incoming negatively charged nucleophiles and maybe somewhat enhanced steric crowding because of the presence of R = nucleoside. The higher β_{nuc} obtained in this work is consistent with the expectation that nucleotidyl transfers as compared with phosphoryl transfers exhibit a more associative transition state based on the decreased repulsive interaction.

2. Catalysis of Hydrolysis of the P–N Bond. Our results can be rationalized by postulating that phosphate mono- and dianion catalyze the hydrolysis of the P–N bond. The corresponding bimolecular rate constants $k_h^{P^-}$ and $k_h^{P^{2-}}$ are included in Table V, and, after statistical correction, provide a Bronsted $\beta = 0.15$. We are not aware of another case where catalysis of the hydrolysis of the P–N bond by general acid or base has been observed.

The observed catalysis prompted us to investigate the possibility of catalysis by the other buffers used in this study. Table VI includes rates obtained for the hydrolysis of 2-MeImpG in the range $5.61 \leq pH \leq 7.29$ as a function of MES concentration with $0.1 \leq [MES] \leq 0.4$ M. No catalysis was observed. However, similar experiments with 2-MeIm buffers in the range $7.23 \leq pH \leq 8.58$ and with $0.05 \leq [2\text{-MeIm}] \leq 0.50$ M indicate a slight catalysis that, interestingly, is pH independent within experimental error. The intercepts (I) and slopes (S) of these buffer plots are included in Table VII. From the slopes we obtain an average $k_h^{2\text{-MeIm}} = 0.61 \times 10^{-2}$ M^{-1} h^{-1}, a rate constant that refers to 2-MeIm irrespective of its ionization state. This catalysis may be rationalized as a medium effect, although it is not clear why it would operate at these relatively low concentrations of buffer ≤0.50 M. Another possibility is that the hydrolysis is catalyzed by both general acid and general base and that the bimolecular rate constants for 2-MeImH$^+$ and 2-MeIm are of similar magnitude.

In a previous report the pK_a^{SH} and the hydrolysis rate constant of 2-MeImpG were determined from the pH dependence of the rates of hydrolysis measured in 2-MeIm buffers, by assuming that these rates would be independent of buffer concentration.[6] The present study shows that even though the catalytic effect of the buffer is weak, it cannot be neglected in analyzing the pH–rate profile. Hence, we used the intercepts (I) of the buffer plots with 2-MeIm as well as the average rate constants with MES buffers in order to refine the previously determined value of pK_a^{SH} of 2-MeImpG. These data lead to the revised $pK_a^{SH} = 7.09$.[14] Since many previously determined rate

Table VII. Kinetics of the Hydrolysis of 2-MeImpG in 2-Methylimidazole Buffers at 37 °C

pH	$[2\text{-MeIm}]_{tot}$, M	10^2k_{obsd}, h^{-1}	10^2I,[a] h^{-1}	10^2S,[a] M^{-1} h^{-1}
7.23	0.05	1.55		
	0.10	1.59		
	0.20	1.66		
	0.30	1.68		
	0.40	1.78		
	0.50	1.76	1.540 ± 0.15	0.50 ● 0.20
7.48	0.10	1.11		
	0.20	1.18		
	0.30	1.27		
	0.40	1.35	1.025 ● 0.10	0.81 ± 0.30
7.62	0.10	0.92		
	0.20	0.96		
	0.30	1.01		
	0.40	1.05	0.875 ● 0.08	0.44 ± 0.18
7.70	0.05	0.699		
	0.10	0.745		
	0.20	0.818		
	0.30	0.900		
	0.40	0.972	0.664 ± 0.06	0.78 ± 0.30
7.82	0.05	0.600		
	0.10	0.65		
	0.20	0.73		
	0.30	0.80		
	0.40	0.85	0.576 ± 0.06	0.72 ± 0.30
7.93	0.05	0.452		
	0.10	0.482		
	0.20	0.529		
	0.30	0.589		
	0.40	0.697	0.409 ± 0.05	0.67 ± 0.27
8.00	0.05	0.392		
	0.10	0.426		
	0.20	0.475		
	0.40	0.561	0.375 ± 0.04	0.47 ± 0.20
8.12	0.05	0.215		
	0.10	0.244		
	0.20	0.335		
	0.40	0.429		
	0.50	0.500	0.190 ± 0.02	0.62 ± 0.25
8.58	0.05	0.128		
	0.10	0.130		
	0.40	0.262		
	0.50	0.321	0.096 ± 0.01	0.44 ± 0.18

[a] I and S are the intercept and slope of a least-squares analysis of the data obtained: k_{obsd} vs total 2-methylimidazole buffer concentration at a specific pH of the solutions; pK_a 8.18 of 2-MeIm at room temperature.

and equilibrium constants depend on this ionization constant we have recalculated them and present the revised constants in Table VIII. Most of the revised values are within 10–30% of the earlier ones, and the conclusions of the earlier work remain unchanged with the following exception: The ratio k_{SH}^{OH} (ImpG)/k_{SH}^{OH} (2-MeImpG), which was calculated under the assumption that the pH-independent hydrolysis proceeds predominantly through the $SH^{\pm} + OH^-$ pathway rather than the $S^- + H_2O$ pathway (Scheme II in ref 6), changes from ≈86 (Table IX in ref 6) to ≈14.2 which reduces the β_{lg} value from ≈−2.17 (Table IX in ref 6) to ≈−1.34. This new value falls now within the "normal" range and allows us to conclude that for both ImpG and 2-MeImpG the $SH^{\pm} + OH^-$ pathway is dominant; in the earlier report we had concluded that for ImpG the $S^- + H_2O$ pathway is dominant.[6] Along the same lines the k_{SH}^{MOH} (ImpG)/k_{SH}^{MOH} (2-MeImpG) ratios for the metal ion catalyzed pathways (Scheme IV in ref 6) are changed from 36 to 9.5 for $M = Mg^{2+}$ and from 40.6 to 10 for $M = Ca^{2+}$, leading to revised $\beta_{lg} = -1.10$ (Mg^{2+}, old value −1.75) and $\beta_{lg} = -1.12$ (Ca^{2+}, old value −1.81).

(14) pK_a^{SH} old value 7.78 in ref 6.

Table VIII. Revised Summary of Rate and Equilibrium Constants for the Hydrolysis of ImpG, 2-MeImpG, 2-MeImpA, N-MeImpG, and 1,2-DiMeImpG in Water in the Absence and Presence of Mg^{2+} (Ca^{2+}) at 37 °C (from Table VIII in Ref 6)

parameter	ImpG	N-MeImpG	2-MeImpG	1,2-diMeImpG	2-MeImpA
pK_a^{SH}	6.01 ± 0.20		7.09 ± 0.20		7.09[c]
K_M, M^{-1}	1.78 ± 0.50		0.58 ± 0.07		0.53 ± 0.07
K_N	0.26 ± 0.03		0.31 ± 0.04		
k_{SH}^{w}, h^{-1}	0.557 ± 0.02		$(3.32 \pm 0.10) \times 10^{-2}$		
k_{SMe}^{w}, h^{-1}		1.76 ± 0.2		0.17 ± 0.03	
k_S^{w}, h^{-1}	$[3.2 \times 10^{-4}]$[a]		$[2.0 \times 10^{-4}]$[a]		
k_{SH}^{OH}, M^{-1} h^{-1}	$\approx 1.49 \times 10^{4}$[b]		$\approx 9.52 \times 10^{2}$[b]		
k_{SMe}^{OH}, M^{-1} h^{-1}		$\geq 3.6 \times 10^{3}$		$\geq 1.3 \times 10^{2}$	
k_S^{OH}, M^{-1} h^{-1}	0.33 ± 0.02		$(2.13 \pm 0.16) \times 10^{-2}$		
k_{SH}^{MOH}, M^{-2} h^{-1}	$(3.9 \pm 0.3) \times 10^{6}$ 7.3×10^{5}[d]		$(4.1 \pm 0.5) \times 10^{5}$ 7.3×10^{4}[d]		$(3.9 \pm 0.5) \times 10^{5}$
k_{SMe}^{MOH}, M^{-2} h^{-1}		7.91×10^{6}		6.37×10^{5}	

[a] Assuming $k_{SH}^{OH}K_w/K_a^{SH} \ll k_S^{w}$, see text; $k_{SH}^{OH} = k_h^{OH}$. [b] Assuming $k_{SH}^{OH}K_w/K_a^{SH} \gg k_S^{w}$, see text; calculated with $K_w = 2.1 \times 10^{-14}$ M^{-2}. [c] Assumed to be the same as for 2-MeImpG. [d] Values refer to Ca^{2+}.

Table IX. Kinetics and Product Distribution of the Reaction of Selected ImpN's in Phosphate Buffers at pH 4.70 ± 0.03 and 37 °C

ImpN	$[phosphate]_{tot}$, M	k_{obsd}, h^{-1}	[5′-NMP]/[5′-NDP][a]
ImpG	0.10	0.796	6.97 ± 0.15
	0.30	1.26	2.28 ± 0.04
	0.50	1.57	1.84 ± 0.01
ImpC	0.10	1.09	6.30 ± 0.10
	0.30	1.50	2.60 ± 0.02
	0.50	1.87	1.94 ± 0.03
2-MeImpC	0.10	5.35×10^{-2}	8.10 ± 0.08
	0.30	7.07×10^{-2}	3.26 ± 0.03
	0.50	8.68×10^{-2}	2.39 ± 0.02

[a] N stands for G = Guanosine in the case of ImpG and N stands for C = Cytidine in ImpC and 2-MeImpC.

3. Reaction of Other ImpN's in Phosphate Buffers. A limited study of the reaction of phosphate with other phosphoimidazolide-activated nucleotides was performed in order to examine whether the reactions observed with 2-MeImpG are general for this type of nucleotides. The results indicate that this is true. Indeed, the rate of disappearance of each ImpG, ImpC, and 2-MeImpC was shown to be dependent on phosphate concentration, and the products were the corresponding mono- and diphosphate nucleotides. Rates of disappearance as well as product ratios for each activated nucleotide as a function of phosphate concentration were monitored only at pH 4.70 and 37 °C with ionic strength of 1.75 (NaCl) and are reported in Table IX. Table III includes an analysis of the data with all three additional ImpN's under the same guidelines as performed with 2-MeImpG. The obtained values for S_k/I_k, I_p, and S_p compare well for the Im and for the 2-MeIm derivatives and confirm that phosphate reacts with these substrates as it does with 2-MeImpG. However, the data are not enough to lead to the determination of bimolecular rate constants. We note that under comparable conditions the rate of P–N bond cleavage in 2-MeImpC is 15–20% faster than in 2-MeImpG. Similarly, the C-derivative is just a trace faster than the G-derivative when comparing ImpC with ImpG. Apparently the change from G to C has an insignificant effect on the rates even though the C-derivatives are partially protonated on the N-3 ($pK_a = 4.5$) at the experimental pH of 4.7.[15] On the other hand there are large rate differences (20-fold or more) between the imidazole and the 2-methylimidazole activating group with both the C- and the G-derivatives because the rate of reaction of the P–N bond depends strongly on the pK_a of the leaving group ($\beta_{lg} = -1.38$ with water as nucleophile for ImpG/2-MeImpG, $pK_a = 7.06$ for Im and 7.95 for 2-MeIm).[6]

Another point worth mentioning is that the product ratios obtained with ImpG and ImpC (Table IX) are about the same within experimental error at all three phosphate concentrations tested. Similarly, the product ratio obtained with 2-MeImpC compares very well with the one with 2-MeImpG at pH 4.65 (Table I). However, the 2-MeIm derivatives exhibit product ratios that are consistently slightly higher than the ones of the Im derivatives. A higher ratio of [5′-NMP]/[5′-NDP] means that with the 2-MeIm derivatives hydrolysis is relatively favored over the phosphate reaction. The effect may possibly be attributed to a somewhat more crowded transition state with the 2-MeIm derivatives because of the additional methyl group. A steric effect may then favor the smaller nucleophile, i.e., water as compared to phosphate monoanion.

4. Formation of 5′-GDP from 2-MeImpG in the Presence of Phosphate: Implications for Chemical Evolution and the Origin of Life. As mentioned in the introduction ImpN's have been used extensively as substrates for the synthesis of RNA-type molecules or polynucleotide analogues. Although ImpN's have been synthesized from polyphosphates and imidazole derivatives under solid phase conditions,[16] the abundance of the ImpN's in a prebiotic environment has been seriously questioned. Their stability/reactivity in the presence of other prebiotically plausible material is also under question. In a previous study we have shown that the rate of hydrolysis of the P-N bond in ImpN's is strongly enhanced in the presence of metal ions, such as Mg^{2+} and Ca^{2+}.[6] The present study shows that ImpN's are also somewhat more labile in the presence of phosphate. However the reaction with phosphate is only significant at concentration several orders of magnitude higher (0.1–0.5 M) than what reasonably can be assumed to have been the concentration on prebiotic Earth. For example, phosphate is approximately 2 μM in the present oceans[17] and, if this is a valid measure for prebiotic oceans, then this "trace" concentration presents no real competition to the hydrolysis reaction. Therefore it seems that, among the reactions studied so far, hydrolysis remains the major pathway for degradation of activated nucleotides.

Another way of looking at the reactivity of ImpN in the presence of large amounts of phosphate (up to 0.5 M)

(15) Protonation of nucleobases: $pK_a = 4.5$ N-3 of cytidine 5′-phosphate, $pK_a = 2.4$ N-7 of guanosine 5′-phosphate: Ts'o, P. O. P., Ed. *Basic Principles in Nucleic Acid Chemistry*; Academic Press: New York, 1974; Vol I, p 462.

(16) Lohrman, R. *J. Mol. Evol.* **1977**, *10*, 137.

(17) The mean phosphate concentration in deep water is 2.25 μmol/kg: Broecker, W. S.; Peng, T.-H. *Tracers in the Sea*; Lamont-Doherty Geological Observatory, Columbia University: Palisades, NY, 1982; p 468.

would be to realize that phosphate transforms part of the ImpN into another activated form of nucleotides, i.e., the nucleoside diphosphate. Even though less activated than the imidazolides, they may, under the proper conditions, also polymerize and lead to polynucleotide synthesis.

Acknowledgment. This research was supported by Grant No NCA 2-474 from the Exobiology Program of the National Aeronautics and Space Administration. We thank Dr. S. Chang from the Planetary Biology Branch of the NASA/Ames Research Center and Prof. C. F. Bernasconi from the Chemistry Department of the University of California at Santa Cruz for providing facilities and for discussions.

Registry No. MES, 4432-31-9; ImpG, 69281-33-0; ImpC, 69673-09-2; GDP, 146-91-8; 2-MeImpG, 80242-42-8; $H_2PO_4^-$, 14066-20-7; HPO_4^{2-}, 14066-19-4; acetic acid, 64-19-7; 2-methylimidazole, 693-98-1.

Enhanced Enantioselectivity of an Enzymatic Reaction by the Sulfur Functional Group. A Simple Preparation of Optically Active β-Hydroxy Nitriles Using a Lipase[1]

Toshiyuki Itoh,* Yumiko Takagi, and Shigenori Nishiyama

Department of Chemistry, Faculty of Education, Okayama University, Okayama 700, Japan

Received May 30, 1990

The enantioselectivity of a lipase-catalyzed hydrolysis was improved by varying the acyl residue into the sulfur functional one, i.e. the β-(phenylthio)- or β-(methylthio)acetoxy group, from acetate or valerate to realize satisfactory resolution of β-hydroxy nitriles using lipase P (*Pseudomonas* sp.).

Introduction

Optically active β-hydroxy nitriles are expected to be useful chiral building blocks for asymmetric synthesis because the cyano group is a functional precursor group of amino and carbonyl groups.[2] Therefore, it is desired to establish a simple method to supply chiral β-hydroxy nitriles that have certain elementary skeletons.[3,4] We have studied the preparation of those compounds using a biocatalytic system such as baker's yeast reduction of the corresponding β-keto nitriles.[5] In these studies, we have encountered a serious problem that limited the number of substrates which could be reduced to the alcohols by bakers' yeast. To obtain various optically active β-hydroxy nitriles, the resolution method using lipases was established for study because these enzymes are stable, cheap, and have broad substrate specificity and stereospecificity.[6] We have tested several kinds of commercially available lipases using 3-(valeroyloxy)butyronitrile as a substrate. However, it has been found that all of the lipases tested lack the capability to resolve the butyronitrile. This shortcoming was generally solved by the discovery of new enzymes with the desired stereochemical features.[6i,j] However, if alternative strategies could be developed for improving enantioselectivity, especially by a chemical modification of the substrate, the usefulness of the biocatalyst could be extended.

In this paper, we describe a simple method of enhancing the enantioselectivity of a lipase-catalyzed hydrolysis by proper modification of the substrates.[1]

Results and Discussion

In 1981, Ohno et al.[7] first reported that the enantioselectivity of pig liver esterase catalyzed hydrolysis of dimethyl β-aminoglutarate was drastically improved by the modification of the substrate, i.e. acylation of the β-amino group. Several reports have been published describing a method of enhancing the stereoselectivity of the enzyme-catalyzed hydrolysis especially by the modification of the substrates.[8] The fact that the enantioselectivity depends on the structure of the acid component of the esters[8a] envisioned us to survey the ester which has a good specificity to a lipase. To determine the combination of the substrates and the lipase to ensure satisfactory results, several kinds of lipases have been tested during 3-hydroxy nitriles as substrates (eq 1).

To a suspension of the substrate, 1, in 0.1 M phosphate buffer (pH 7.2) was added the lipase (50 wt % of the substrate), which was stirred at 40 °C. Progress of the reaction was monitored by silica gel thin-layer chromatography (TLC). The reaction was stopped when the spots due to the ester and the alcohol became the same size. The reaction mixture was extracted with ethyl acetate and separated by silica gel TLC with the conversion ratio being determined by ^1H NMR analysis. Optical purity of the hydrolyzed alcohol, 2, was determined by ^1H NMR analysis

(1) Preliminary accounts have appeared: (a) Itoh, T.; Takagi, Y. *Chem. Lett.* **1989**, 1505. (b) Itoh, T.; Kuroda, K.; Tomosada, M.; Takagi, Y. *J. Org. Chem.*, in press.

(2) Tennant, G. *Comprehensive Organic Chemistry*; Barton, D., Ollis, D., Eds.; Pergamon Press: 1979; Vol. 2, p 385.

(3) Levene, P. A.; Haller, H. L. *J. Biol. Chem.* **1928**, *76*, 415.

(4) For the racemic one, see: (a) Vinick, F. J.; Pan, Y.; Gschwend, H. *Tetrahedron Lett.* **1978**, 4221. (b) Wade, P. A.; Pilay, M. K. *J. Org. Chem.* **1981**, *46*, 5435. (c) Kuwahara, T.; Takahashi, H. *Bull. Chem. Soc. Jpn.* **1969**, *42*, 1745.

(5) (a) Itoh, T.; Takagi, Y.; Fujisawa, T. *Tetrahedron Lett.* **1989**, *30*, 3811. (b) Itoh, T.; Fukuda, T.; Fujisawa, T. *Bull. Chem. Soc. Jpn.* **1989**, *62*, 3851.

(6) Recent review, see: (a) Crout, D. H. G.; Christen, M. *Modern Synthetic Methods 1989*; Scheffold, R., Ed.; Springer Verlag: New York, 1989; pp 1-114. (b) Chen, C.-S.; Sih, C. J. *Angew. Chem., Int. Ed. Engl.* **1989**, *28*, 695. (c) Wong, Y.-F.; Wong, C.-H. *J. Org. Chem.* **1988**, *53*, 3129. For recent other examples, see: (d) Von der Osten, C. H.; Sinskey, A. J.; Barbas, C. F. III; Pederson, R. L.; Wang, Y.-F.; Wong, C.-H. *J. Am. Chem. Soc.* **1989**, *111*, 3924. (e) Ngooi, T. K.; Scilimati, A.; Guo, Z.-W.; Sih, C. J. *J. Org. Chem.* **1989**, *54*, 911. (f) Berinakatti, H. S.; Benerji, A. A.; Newadkar, R. V. *Ibid.* **1989**, *54*, 2453. (g) Gutman, A. L.; Brardo, T. *J. Org. Chem.* **1989**, *54*, 4263. (h) Gutman, A. L.; Brardo, T. *Ibid.* **1989**, *54*, 5645. (i) Yamazaki, T.; Ichikawa, S.; Kitazume, T. *J. Chem. Soc., Chem. Commun.* **1989**, 934. (j) Yamada, H.; Ohsawa, S.; Sugai, T.; Ohta, H.; Yoshikawa, S. *Chem. Lett.* **1989**, 1775. (k) Feichter, C.; Faber, K.; Griengel, H. *Tetrahedron Lett.* **1989**, *30*, 551. (l) Hiratake, J.; Yamamoto, K.; Yamamoto, Y.; Oda. J. *Ibid.* **1989**, *30*, 1555. (m) Hirai, K.; Miyakoshi, S.; Naito, A. *Ibid.* **1989**, *30*, 2553. (n) Guanti, G.; Banfi, L.; Narisano, E. *Ibid.* **1989**, *30*, 2697. (o) Burgess, K.; Henderson, I. *Ibid.* **1989**, *30*, 3633. (p) Burgess, K.; Jennings, L. D. *J. Org. Chem.* **1990**, *55*, 1138. (q) Babiak, K. A.; Ng, J. S.; Dygos, J. H.; Weyker, C. L.; Wang, Y.-F.; Wong, C.-H. *Ibid.* **1990**, *55*, 3377. (r) Cregge, R. J.; Wagner, E. R.; Freedman, J.; Margolin, A. L. *Ibid.* **1990**, *55*, 4237.

(7) Ohno, M.; Kobayashi, S.; Iimori, T.; Fong, Y.; Izawa, T. *J. Am. Chem. Soc.* **1981**, *103*, 2405.

(8) (a) Ltu, Q.-M.; Peddy, D. R.; Sih, C. J. *Tetrahedron Lett.* **1986**, *27*, 5203. (b) Adachi, K.; Kobayashi, S.; Ohno, M. *Chimica* **1986**, *40*, 311.

0022-3263/91/1956-1521$02.50/0